

## **A new type acetylene gas sensor based on hollow heterostructure**

Ying Lin <sup>a</sup>, Chao Li <sup>a</sup>, Wei Wei <sup>a</sup>, Yujia Li <sup>b</sup>, Shanpeng Wen <sup>a,\*</sup>, Dongming Sun <sup>a</sup>, Yu Chen <sup>c,\*</sup>, Shengping

Ruan <sup>b,\*</sup>

<sup>a</sup> State Key Laboratory on Integrated Optoelectronics, Jilin University, Changchun 130012, P. R. China.

<sup>b</sup> College of Electronic Science and Engineering, Jilin University, Changchun 130012, P. R. China.

<sup>c</sup> Institute of Semiconductors, Chinese Academy of Sciences, Beijing 100083, China.

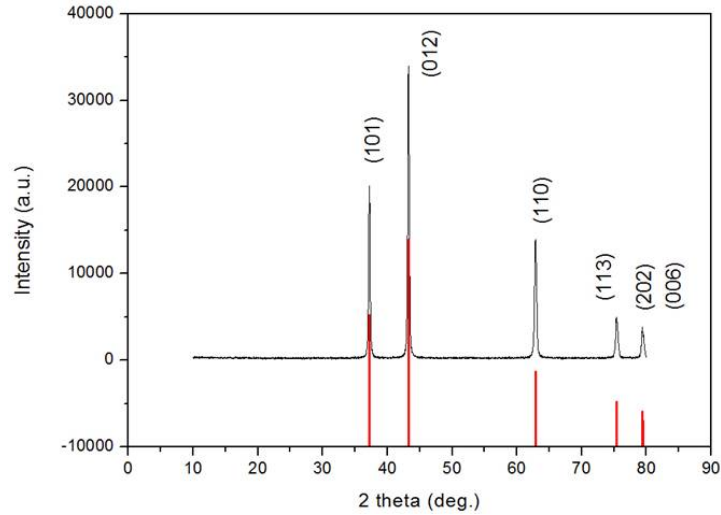


Fig.S1. XRD patterns of NiO by the first hydrothermal.

In Fig.S1 the peaks appeared at  $37.28^\circ$ ,  $43.28^\circ$ ,  $62.88^\circ$ ,  $75.4^\circ$ ,  $79.4^\circ$  and  $79.46^\circ$  were corresponding to (101), (012), (104), (113), (202) and (006), respectively, crystal planes of the nickel oxide (JCPDS card no. 44-1159). Therefore, it demonstrated that the NiO material was successfully synthesized by the first hydrothermal method.

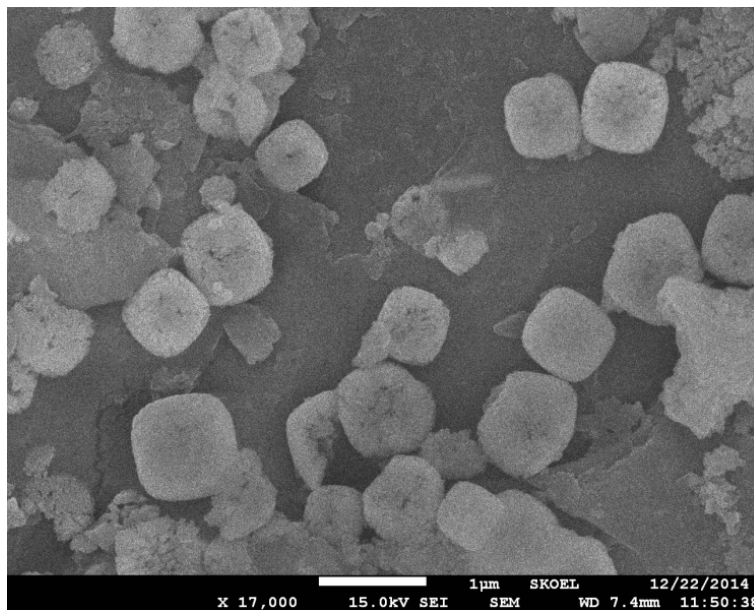


Fig. S2. SEM images of the NiO nanocubes.

In Fig.S2 it can be seen that the NiO nanocubes with the diameter of about 800 nm were synthesized by the first hydrothermal method.

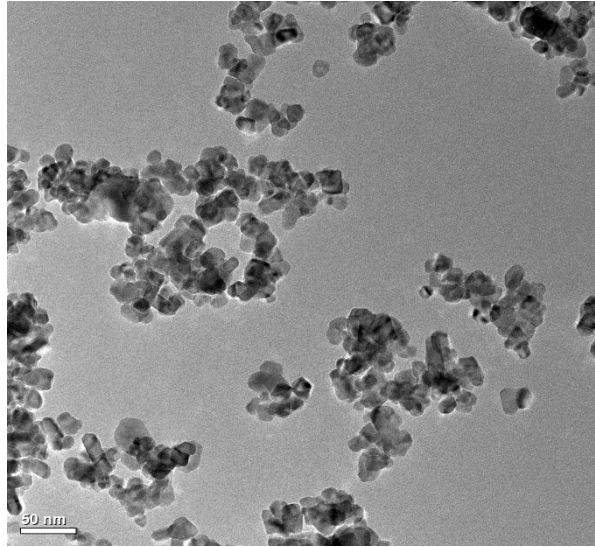


Fig. S3. TEM images of the pure SnO<sub>2</sub> nanoparticles.

As shown in Fig. S3, the TEM image showed the pure SnO<sub>2</sub> was composite of uniform nanoparticles with a diameter of about 30 nm. And the nanoparticles were not the hollow structure.

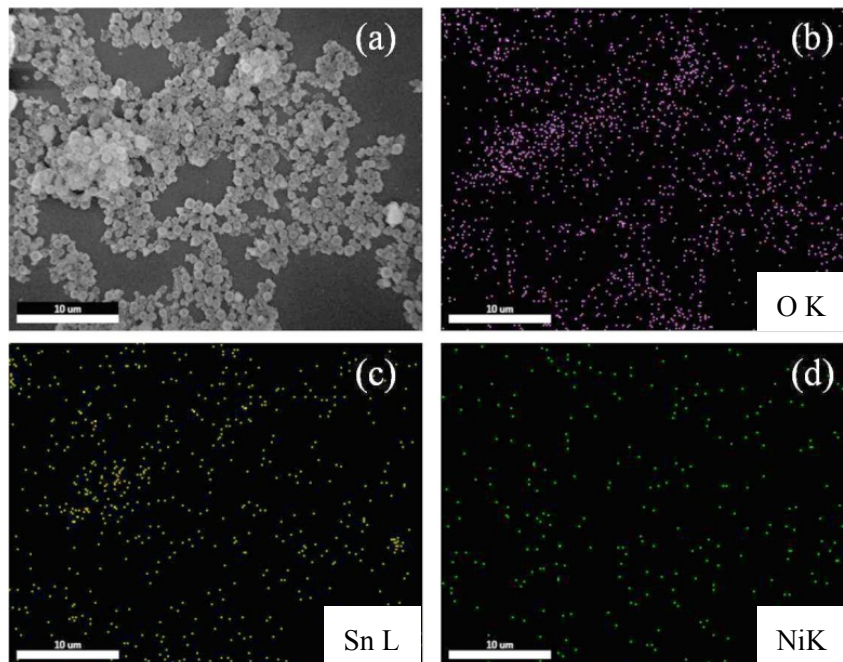


Fig. S4 SEM and EDX mapping images of hollow NiO/SnO<sub>2</sub> composite

Fig. S4 showed the SEM and EDX mapping of all elements in the hollow NiO/SnO<sub>2</sub> heterostructure. It could be seen that O, Sn and Ni were quite evenly distributed over the area. Therefore, it is reasonable to believe that SnO<sub>2</sub> was wrapped on the surface of NiO nanocubes.

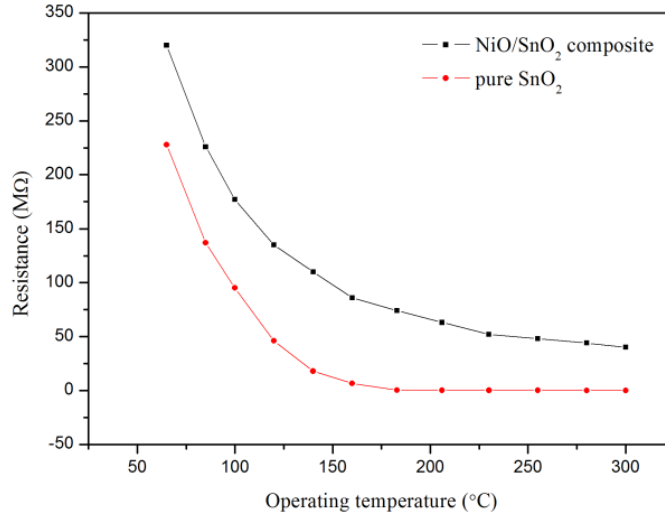


Fig. S5 The relation between resistance ( in air ) and the operating temperature of the sensors

The relation between resistance and the operating temperature of the sensors ( in air ) was shown in Fig. S5. In region of 65 °C ~ 180 °C, the resistances of the NiO/SnO<sub>2</sub> composite and the pure SnO<sub>2</sub> decreased dramatically. In the region of 180 °C ~ 300 °C, the change in resistance was very small. As a result, the atmospherical resistance of the hollow NiO/SnO<sub>2</sub> heterostructures was larger than that of pure SnO<sub>2</sub> at each tested operating temperature.

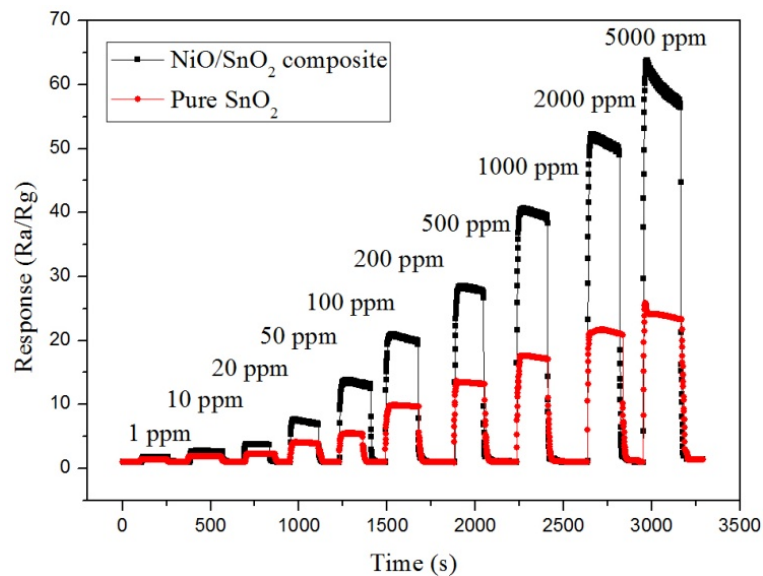


Fig.S6. Curves of sensors' responses versus acetylene concentrations from 1 ppm to 5000 ppm.

Fig. S6 presented the response-recovery curves in the range of 1-5000 ppm concentrations of acetylene. The minimum detection limit was 1 ppm corresponding to the response of 1.8.

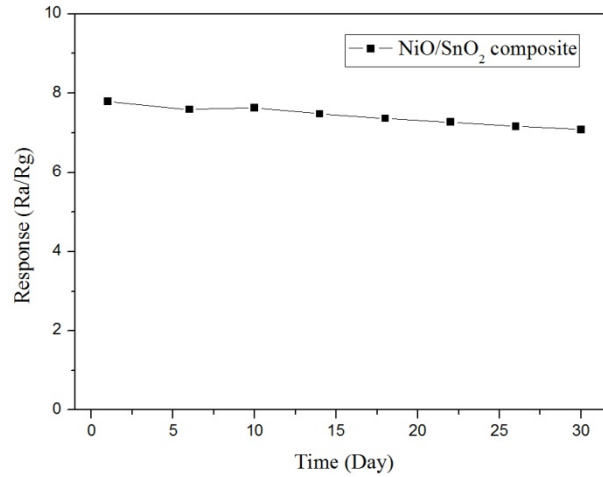


Fig. S7. The stability of the NiO/SnO<sub>2</sub> composite to 50 ppm acetylene.

Fig. S7 displayed the stability of the hollow NiO/SnO<sub>2</sub> gas sensor which was measured to 50 ppm acetylene at 206 °C for 30 days. In the experiments, the sensor was tested every two days. The results exhibited that the response changed little during the times. It was obvious that the sensor based on the hollow NiO/SnO<sub>2</sub> gas sensor had a good stability.